Numerical modelling of intergranular fracture in polycrystalline materials and grain size effects

M. Paggi
Department of Structural and Geotechnical Engineering, Politecnico di Torino, Torino (Italy)
marco.paggi@polito.it

P. Wriggers
Institut für Kontinuumsmechanik, Leibniz Universität Hannover, Hannover (Germany)
wriggers@ikm.uni-hannover.de

ABSTRACT. In this paper, the phenomenon of intergranular fracture in polycrystalline materials is investigated using a nonlinear fracture mechanics approach. The nonlocal cohesive zone model (CZM) for finite thickness interfaces recently proposed by the present authors is used to describe the phenomenon of grain boundary separation. From the modelling point of view, considering the dependency of the grain boundary thickness on the grain size observed in polycrystals, a distribution of interface thicknesses is obtained. Since the shape and the parameters of the nonlocal CZM depend on the interface thickness, a distribution of interface fracture energies is obtained as a consequence of the randomness of the material microstructure. Using these data, fracture mechanics simulations are performed and the homogenized stress-strain curves of 2D representative volume elements (RVEs) are computed. Failure is the result of a diffuse microcrack pattern leading to a main macroscopic crack after coalescence, in good agreement with the experimental observation. Finally, testing microstructures characterized by different average grain sizes, the computed peak stresses are found to be dependent on the grain size, in agreement with the trend expected according to the Hall-Petch law.

SOMMARIO. In questo articolo, il fenomeno della frattura intergranulare nei material policristallini è studiato mediante un approccio di meccanica della frattura non lineare. Il modello non locale di frattura coesiva per interfacce con spessore finito recentemente proposto dai presenti autori è impiegato per descrivere il fenomeno di separazione ai bordi di grano. Da un punto di vista modellistico, considerando la dipendenza dello spessore dei bordi di grano dalla dimensione del grano stesso, si è ottenuta una distribuzione delle proprietà meccaniche delle interfacce. Essendo la forma ed i parametri del modello non locale della frattura coesiva dipendenti dallo spessore dell'interfaccia, si ottiene una distribuzione di energie di frattura come conseguenza della variabilità statistica della microstruttura del materiale. Usando tali dati si conducono simulazioni di meccanica della frattura su elementi di volumi rappresentativi (RVE) in 2D e si determinano le rispettive curve di tensione-deformazione. La frattura è il risultato di un insieme di microfessure diffuse che danno luogo alla propagazione di una fessura macroscopica principale, in ottimo accordo con quanto osservato sperimentalmente. Infine, testando microstrutture dotate di diversi diametri medi dei grani, si osserva come le tensioni di picco siano dipendenti dal diametro del grano, secondo un trend in accordo con la legge di Hall e Petch.

KEYWORDS. Nonlocal cohesive zone model; Nonlinear and stochastic fracture mechanics; Finite thickness interfaces; Finite elements; Polycrystalline materials.

INTRODUCTION

Polycrystalline materials present heterogeneous microstructures where polyhedral grains are separated by interfaces. A typical scanning electron microscope (SEM) image of these microstructures is shown in Fig. 1(a). The different colours of the crystals indicate their different crystallographic orientations. The mechanical behaviour is strongly affected by the grain boundaries which govern the strength, the toughness and the ductility of the material. These properties are of paramount importance in forming processes and for the design of super-hard materials. As a general trend, the smaller the grain, the higher the material strength and the hardness. Interfaces are also important in conduction processes. In this case, however, they should be viewed as defects and the material conductivity of single crystalline materials is usually much higher than that of their polycrystalline counterparts.

Fracture in polycrystalline materials can be schematically classified according to two different types: *intergranular* and *transgranular*. The former mode of fracture corresponds to the decohesion of the grains along the interfaces. Correspondingly, the material response is quite brittle. The latter is characterized by a propagation of cracks into the grains, with the occurrence of high plastic deformations leading to a much more ductile response. In spite of the fact that failure is often the result of a combination of these two modes of fracture, it is instructive to investigate each mode separately and understand the underlying mechanisms. In the present study, attention is paid to intergranular fracture, which is typically observed in brittle polycrystals. During a tensile test, microcracks develop at the grain boundaries (see Fig. 1(b) taken from [1]). At a certain deformation level, the microcracks coalescence and lead to the final failure with the propagation of a single main crack. Correspondingly, the stress-strain curve reaches a maximum and a sudden loss of load carrying capacity takes place.

In order to investigate the effect of interfaces on the mechanical response of polycrystalline materials, a nonlinear fracture mechanics model is herein proposed. Intergranular fracture is depicted as a phenomenon of progressive separation at the grain boundaries governed by a nonlinear traction-separation law, or cohesive zone model (CZM). In this context, the finite thickness properties of interfaces are suitably taken into account by using the nonlocal CZM recently proposed in [2, 3] and briefly summarized in the next section. Virtual tensile tests of representative volume elements (RVEs) of material microstructures are carried out in order to simulate the phenomena of crack nucleation, coalescence and strain localization. Finally, grain size effects are investigated by changing the average grain size of the polycrystalline material and computing the peak stress of the simulated stress-strain curves. As it will be shown, numerical results are in agreement with the trend expected by the Hall-Petch law. This result confirms that fracture mechanics of interfaces is one of the most important factors governing the strength of polycrystalline materials.

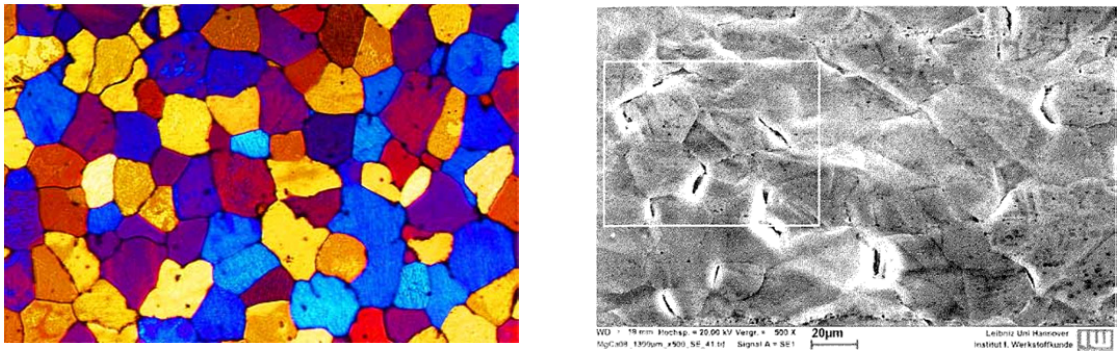

(a) SEM image of the microstructure (b) Microcracks observed during a tensile test

Figure 1: SEM images of brittle polycrystalline materials showing microcracks (courtesy of Dr. Ing. M. Schaper [1]).

A NONLOCAL COHESIVE ZONE MODEL FOR INTERFACE FRACTURE

Polycrystals are an important example of a material with finite thickness interfaces. In particular, examining the materials science literature [4], a power-law dependency of the interface thickness on the grain diameter has been noticed. Figure 2 shows the relation proposed in [4], where the grain diameter is computed as the mean diameter

of two grains sharing the same interface. A criterion of equivalence of cross-sectional areas is used to compute the diameter d of a polyhedral grain. Although the interface thickness l_2 is approximately one order of magnitude smaller than the grain diameter, as shown in Fig. 2(b), its simplification as a zero-thickness region, also called *boundary layer*, is not always possible. Numerical simulations considering an elasto-plastic behaviour of the interfaces suggest that the ductility of the material is strongly affected by these finite thickness regions [4].

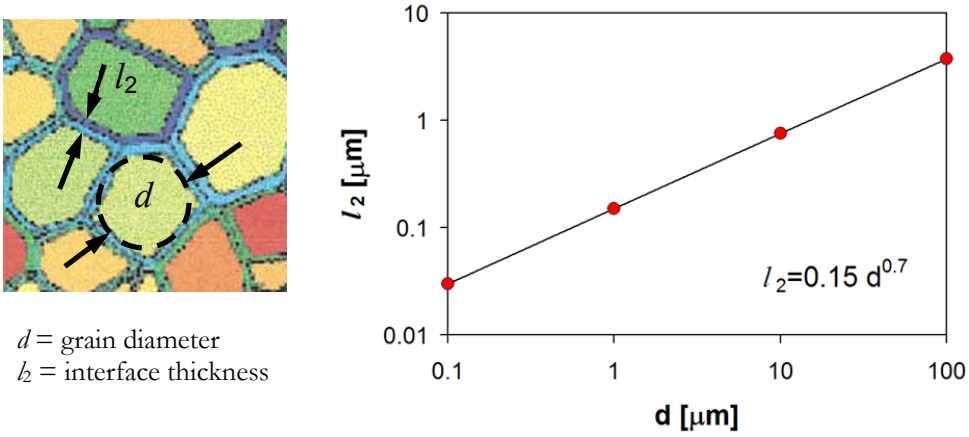

Figure 2: Dependency of the interface thickness on the grain diameter according to the relation proposed in [4].

In order to simplify the real material microstructure by considering a finite element discretization with zero-thickness interfaces, a suitable interface constitutive law has to be used (see [5-16] for a wide range of problems modelled using CZMs). Here, we consider the nonlocal CZM recently proposed in [2] for finite thickness interfaces. The traction-separation relations that describe the nonlinear response of the interface are the following:

$$\tau = \tau_e \frac{1-D}{D} \frac{g_T}{\psi_e} \tag{1a}$$

$$\sigma = \sigma_e \frac{1-D}{D} \frac{g_N}{\delta_e} \tag{1b}$$

where τ and σ are the tangential and normal cohesive tractions. The parameters g_T and g_N denote, respectively, the tangential and normal anelastic displacements evaluated at the boundaries of the finite thickness interface. Finally, τ_e and σ_e are the threshold values of the cohesive tractions for the onset of damage that correspond to the global tangential and normal displacements ψ_e and δ_e of the interface region. The damage variable D $(0 \le D \le 1)$ is computed as follows:

$$D = \left[\left(\frac{w}{w_c} \right)^2 + \left(\frac{u}{u_c} \right)^2 \right]^{\alpha/2} \tag{2}$$

where w_c and u_c are material parameters analogous to the critical opening and sliding displacements l_{Nc} and l_{Tc} used in standard CZMs [9] and α is a free parameter. The displacements u and w are given by:

$$u = g_T - \psi_e + \tau \frac{l_2}{G_2} \tag{3a}$$

$$w = g_N - \delta_e + \sigma \frac{l_2}{E_2} \tag{3b}$$

where l_2 is the thickness of the interface, E_2 and G_2 are the initially undamaged normal and tangential elastic moduli of the interface material. Changing the parameter α, different shapes of the CZM can be obtained, as shown in Fig. 3 for a

Mode I problem. Similar considerations apply for Mode Mixity. For more details about the calibration of the model parameters using molecular dynamics simulations, the readers are referred to [2].

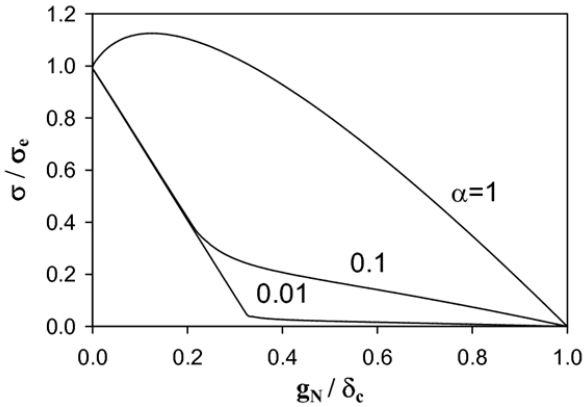

Figure 3: Shape of the Mode I nonlocal CZM as a function of α.

This nonlocal CZM has been implemented in the FE code FEAP [17] using zero-thickness interface elements, see [3] for more details about the computational aspects. The anelastic relative displacements g_N and g_T are the main input of the element subroutine and are obtained as the difference between the normal and tangential displacements of the nodes of the finite elements of the continuum opposite to the shared interface.

The residual vector and the tangent stiffness matrix of the interface element are computed by linearizing the corresponding weak form using a Newton-Raphson algorithm. Due to the implicit form of the CZM in Eq. (1), since the damage variable D on the r.h.s. of Eq. (1) is a function of the unknown cohesive tractions through Eqs. (2) and (3), a nested Newton-Raphson iterative scheme is used in to compute the cohesive tractions. A quadratic convergence is achieved, as shown in Fig. 4 for a Mode I problem.

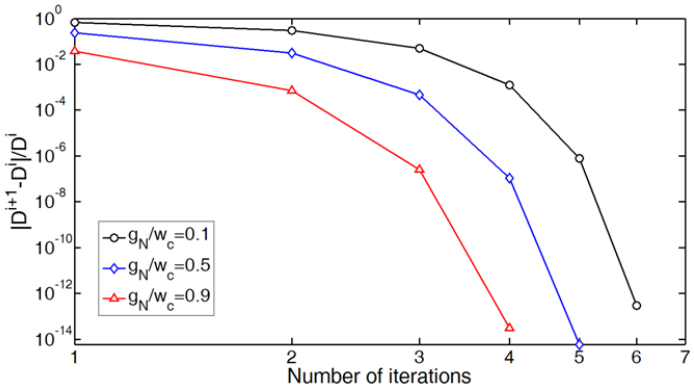

Figure 4: Quadratic convergence of the Newton-Raphson method used for the computation of the cohesive tractions, for three different values of g_N / w_c and for $g_T / u_c = 0$.

APPLICATIONS TO POLYCRYSTALLINE MATERIALS

The proposed nonlocal CZM for finite thickness interfaces is applied to the polycrystalline material microstructure of Copper analyzed in [1] and depicted in Fig. 5. From this input geometry, the grain size distribution, shown in Fig. 6(a), can be computed. The average grain diameter is 1 μm and its r.m.s. deviation is 0.26 μm. The interface thickness distribution is also computed and shown in Fig. 6(b).

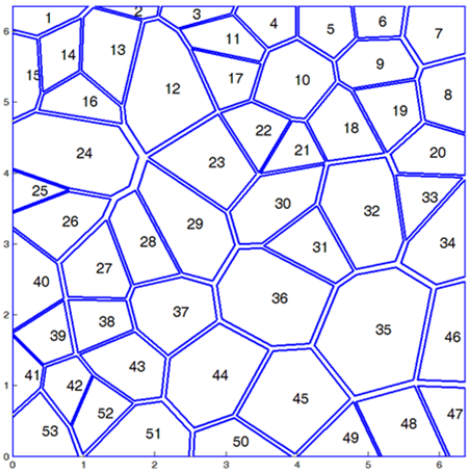

Figure 5: Material microstructure of polycrystalline Copper numerically analyzed in this work.

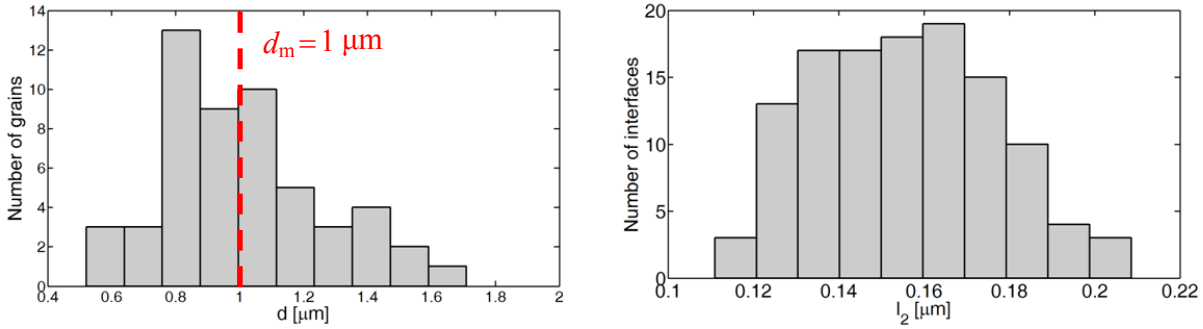

(a) (b)

Figure 6: (a) Grain size distribution and (b) interface thickness distribution of the microstructure shown in Fig. 5.

According to the thickness-dependent nonlocal CZM summarized in the previous section, the distribution of the Mode I interface fracture energy, represented by the area below the Mode I traction-separation curve, is obtained and shown in Fig. 7. It is interesting to note that the distribution of Mode I interface fracture energies for the present case (dots in Fig. 7) is better approximated by a Gaussian than by a Weibull distribution (see the probability plots in Fig. 7(a) and 7(b), where the Gaussian and Weibull distributions computed from the sample population are depicted with dashed-dotted lines). This is in general agreement with ductility of the material microstructure herein examined. Incidentally, we note that the Weibull modulus for these data is equal to 7.7, which is in agreement with the typical range of variation between 5 and 10 found in polycrystals [16]. This can be considered as an indirect experimental confirmation of the fact that the interface thickness distribution is responsible for the interface fracture energy distribution.

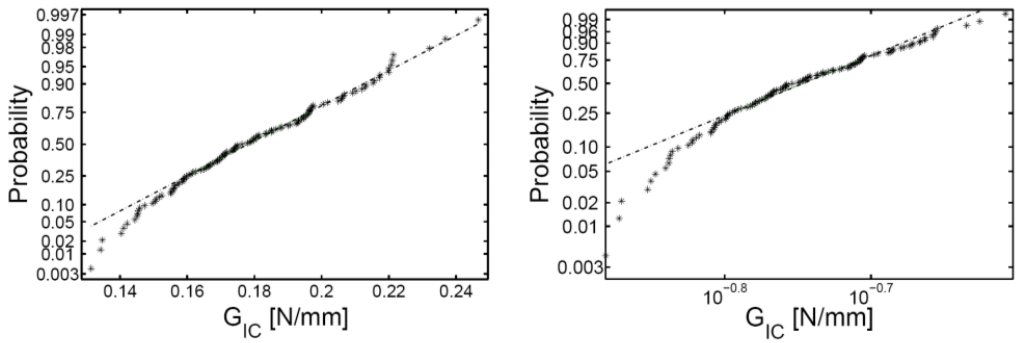

(a) Gaussian probability plot (b) Weibull probability plot

Figure 7: Mode I interface fracture energy distribution and comparison with the Gaussian and the Weibull distributions.

The parameters of the average Mode I traction-separation curve, corresponding to an average value of l_2=0.15 μm, were selected in order to obtain an average Mode I fracture energy of 0.18 N/mm and a peak stress of 500 N/mm², as suggested in [6] for polycrystalline interfaces (see the corresponding curve in Fig. 8 with solid line). More specifically, $\delta_c = \psi_c = 0.53\,\mu\text{m}$, $\sigma_e = \tau_c = 500\,\text{N/mm}^2$, $E_2 = 110\times10^3\,\text{N/mm}^2$ were set for the grains, and the parameter α was selected as 0.0035. Alternatively, the parameters of the nonlocal CZM can be tuned to fit MD simulations, as illustrated in [2]. Interestingly, the shape of the nonlocal CZM can be matched with a good approximation with the standard CZM proposed by Tvergaard [9]. It is superimposed to Fig. 8 with dashed line and has the same Mode I fracture energy as our model.

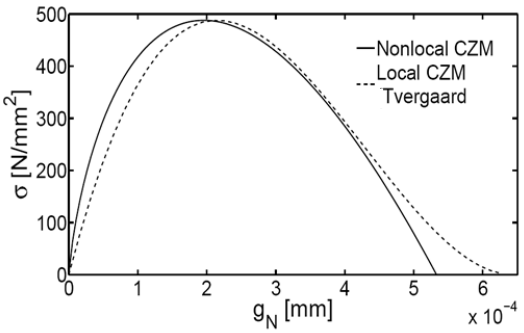

Figure 8: Shape of the nonlocal CZM (average curve) used for the fracture simulations and that of the Tvergaard [9] model with the same average fracture energy.

To quantify the effect of using the nonlocal CZM with random properties instead of the Tvergaard CZM with the same properties for all the interfaces, we consider an elastic modulus of the grains equal to $E_1 = 110\times10^3\,\text{N/mm}^2$ and a Poisson ratio equal to ν=0.3 for all the grains. The material microstructure shown in Fig. 5 is first simplified by augmenting the size of the grains, according to the procedure outlined in [2]. After this preliminary operation, each grain is meshed with constant strain triangular elements according to a Delauney triangulation. Then, zero-thickness interface elements governed by the thickness-dependent nonlocal CZM are placed along the grain boundaries. The size of the finite elements used for discretizing the continuum has been chosen in order to be one order of magnitude smaller than the process zone size, estimated according to the method suggested in [16].

The Dirichlet boundary conditions imposed on the model are selected to reproduce a tensile test, i.e., the nodes pertaining to the left vertical boundary are restrained to the horizontal displacements, whereas horizontal displacement are imposed on the nodes of the vertical boundary on the right. A Newton-Raphson solution scheme is adopted to solve the nonlinear boundary value problem at each step. The tolerance for the internal Newton-Raphson loop used to compute the residual and the tangent stiffness matrix of the interface elements is chosen as 1×10^{-12}.

In Fig. 9, the evolution of the crack pattern using the Tvergaard CZM with the same parameters for all the interfaces (pictures at the top) is compared with that obtained using the nonlocal CZM and random fracture properties (pictures at the bottom), for three different deformation levels, ε=0.100, 0.115 and 0.124. The last deformation level corresponds to the final failure of the samples. Dashed lines correspond to fictitious cracks, i.e., microcracks where cohesive tractions are still acting. Solid lines correspond to the interfaces with D=1, i.e., real stress-free microcracks. The evolution of cohesive microcracks is widely distributed in both cases. At a certain point, when the microcracks coalescence into a single rough macrocrack, a phenomenon of strain localization takes place. The cohesive microcracks far from the main crack experience a stress relief, whereas the deformation accumulates on the main crack. This is well evidenced by the fact that microcracks (dashed segments) almost disappear at the deformation level of 0.124. The final crack pattern in case of uniform interface fracture properties appears to be characterized by a single main crack. On the contrary, using the nonlocal CZM with thickness dependent fracture properties, we obtain a separation of some grains and a more diffuse crack pattern, which is often found in experiments.

The homogenized stress-strain responses of the composite cell are compared in Fig. 10. The homogenized stress is computed by summing the horizontal reactions of the constrained nodes on the vertical boundary on the right, and dividing it for its length. The use of the Tvergaard model (local CZM with uniform interface fracture properties) leads to a higher peak stress than using the proposed nonlocal CZM. This is mainly due to the prevalence of subvertical microcracks

subjected to pure Mode I. In both cases, the final failure of the sample is characterized by a sudden stress drop in the stress-strain diagram, probably due to a snap-back instability, typical of cohesive solids.

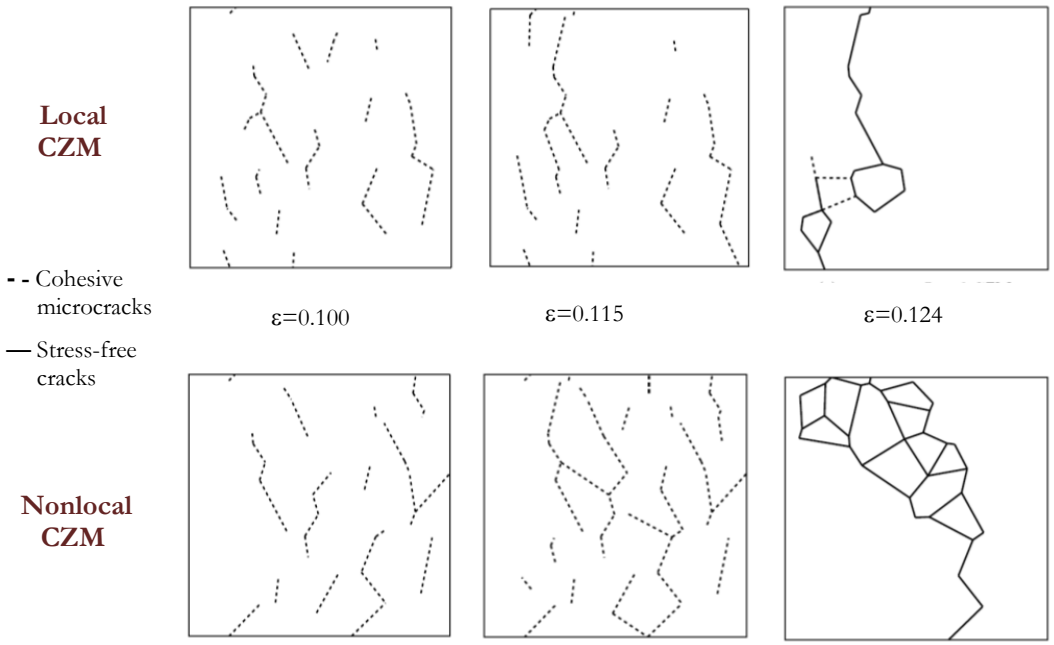

Figure 9: Crack patterns (cohesive microcracks with dashed line and stress-free cracks with solid line) for different strain levels.

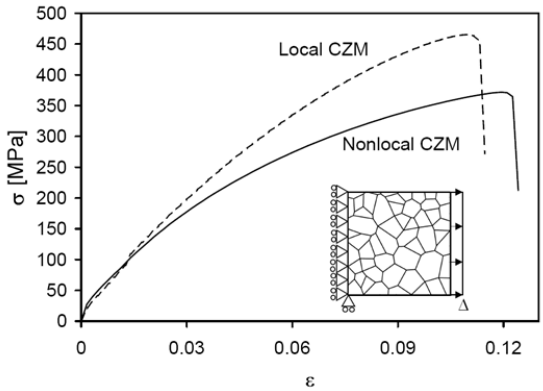

Figure 10: Homogenized stress-strain curve. The nonlocal CZM response (with stochastic distribution of interface properties) is compared with the prediction of the local CZM by Tvergaard with the same fracture energy for all the interfaces.

The proposed nonlocal CZM is also able to capture the grain-size effects on the tensile strength. In polycrystalline materials, the tensile strength significantly depends on the grain size. An empirical correlation was proposed by Hall [18] and Petch [19], suggesting that the tensile strength is in general proportional to the inverse of the square root of the grain size at the microscale.

To assess the capability of the proposed nonlocal CZM to capture this effect, we consider different material microstructures, replicas of that in Fig. 5, obtained by rescaling the diameters of the grains. Since the interface thicknesses depend on the grain size according to the power-law relation displayed in Fig. 2(b), the rescaled geometries are not self-similar. As a consequence, the distribution of the interface fracture parameters will also depend on the grain size. The Mode I fracture energy distributions corresponding to microstructures with average grain sizes of 0.1μm, 1μm and 10μm are shown in Fig. 11. The shapes of the CZM for the three cases are similar to that shown in Fig. 8. In particular, the maximum cohesive stress of the curves changes, whereas the critical separation remains the same. The average fracture

energy for the three cases is equal to 0.8974 N/mm, 0.1794 N/mm and 0.0361 N/mm, for d_m=0.1μm, 1μm and 10μm, respectively. The r.m.s values are equal to 0.122 N/mm, 0.024 N/mm and 0.005 N/mm, respectively.

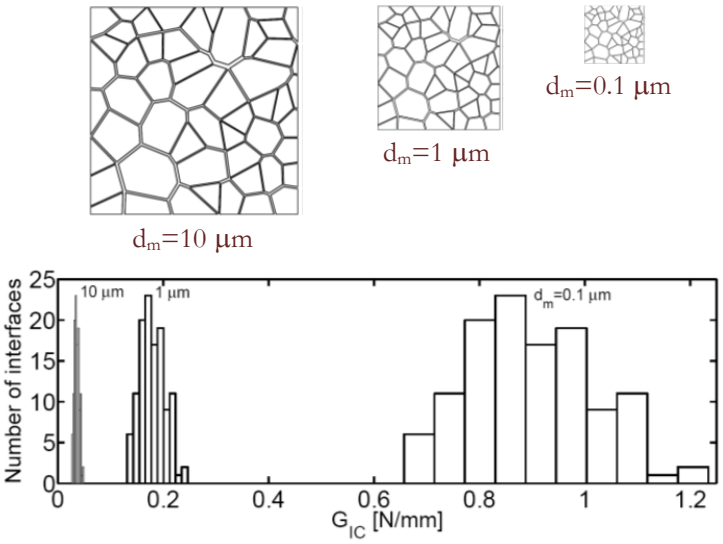

Figure 11: Distribution of interface fracture energies for three different average grain sizes.

The peak stress of the stress-strain curves, obtained from tensile test simulations on the different cases, considering also d_m=0.5μm, 2μm and 5μm in addition to 0.1μm, 1μm and 10μm, are shown in Fig. 12 vs. the grain diameter. The FE simulations lead to a peak stress which is a decreasing function of the grain size, in general agreement with the Hall-Petch relation that is superimposed to the same data in Fig. 12 by the dashed line. Therefore, the nonlocal CZM is fully able to reproduce the scaling of the tensile strength through the variation of fracture mechanics parameters connected to the variation of the interface thicknesses with the grain size. These numerical results imply that thicker interfaces are weaker than the thinner ones.

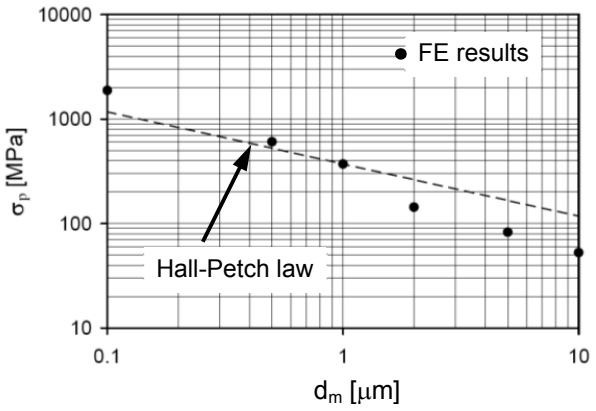

Figure 12: Numerically predicted vs. experimentally obtained peak stress vs. average grain size.

CONCLUSIONS

In this paper, intergranular fracture in polycrystalline materials has been numerically investigated using finite elements. The main novelty with respect to previous contributions based on CZMs is represented by the use of a more sophisticated CZM whose properties (shape, fracture energy, peak stress) depend on the finite thickness of the interface. This is particularly suitable for polycrystalline materials in the micro-scale range, where the grain boundary thickness is not negligible and has an important role. The proposed nonlocal CZM is based on continuum damage

mechanics through the introduction of a damage variable that reduces the elastic modulus of the interface material. This approach allows us to perform an upscaling of the complex nonlinear mechanisms occurring in the interface region. The parameters entering the damage formulation can be tuned according to simple axial and shear tests to be performed on RVEs of the interface microstructure. This strategy has the great advantage of avoiding computationally expensive multiscale simulations based on the FE^2 method which requires, for each Gauss point, a micromechanical computation of the response of a lower scale RVE with a complete description of its constitutive nonlinearities [20-22]. Possible applications to fiber-reinforced interfaces and polymeric interfaces are therefore envisaged, with a tuning of the damage evolution law depending on the actual forms of nonlinearities present in those materials.
Finally, regarding the grain size effects on the tensile strength of polycrystals, it has to be remarked that an inversion of the trend suggested by Hall and Petch has been observed at the nanoscale. Although a different description of the material has probably to be invoked, using molecular dynamics simulations instead of continuum mechanics, our proposed model may provide an insight into this debated problem. The results obtained in the present study show that the thinner the interface, the higher its fracture energy. As a result, the tensile strength of the material increases by refining the material microstructure. This suggests that an inversion of the Hall-Petch law may occur in case of thicker interfaces at the nanoscale. Experimental results seem to confirm this predicted trend. In fact, data in [23] show that the grain boundary thickness tends to vanish at the nanoscale. However, the percentage of atoms at the grain vertices, the so called *triple junctions*, drastically increases. As a result, the volumetric content of the all interface atoms (the sum of the atoms belonging to triple junctions and those belonging to grain boundaries), is much higher than that suggested by the scaling law holding at the microscale and shown in Fig. 2.

ACKNOWLEDGEMENTS

The support of AIT, MIUR and DAAD to the Vigoni 2011-2012 project "3D Modelling of fracture in polycrystalline materials" is gratefully acknowledged. MP would also like to thank the Alexander von Humboldt Foundation for supporting his research fellowship at the Institut für Kontinuumsmechanik, Leibniz Universität Hannover (Hannover, Germany) from February 1, 2010, to January 31, 2011.

REFERENCES

[1] P. Kustra, A. Milenin, M. Schaper, A. Gridin, Computer Methods in Materials Science, 9 (2009) 207.
[2] M. Paggi, P. Wriggers, Computational Materials Science, 50 (2011) 1625.
[3] M. Paggi, P. Wriggers, Computational Materials Science, 50 (2011) 1634.
[4] D.J. Benson, H.-H. Fu, M.A. Meyers, Materials Science and Engineering A, 319–321 (2001) 854.
[5] Yan-Qing Wu, Hui-Ji Shi, Ke-Shi Zhang, Hsien-Yang Yeh, International Journal of Solids and Structures, 43 (2006) 4546.
[6] T. Luther, C. Könke, Engineering Fracture Mechanics, 76 (2009) 2332.
[7] P.D. Zavattieri, P.V. Raghuram, H.D. Espinosa, Journal of the Mechanics and Physics of Solids, 49 (2001) 27.
[8] G. Beer, International Journal for Numerical Methods in Engineering, 21 (1985) 585.
[9] V. Tvergaard, Material Science and Engineering A, 107 (1990) 23.
[10] N. Point, E. Sacco, International Journal of Fracture, 79 (1996) 225.
[11] M. Ortiz, A. Pandolfi, International Journal for Numerical Methods in Engineering, 44 (1999) 1267.
[12] J. Segurado, J. Llorca, International Journal of Solids and Structures, 41 (2005) 2977.
[13] S. Li, M.D. Thouless, A.M. Waas, J.A. Schroeder, P.D. Zavattieri, Composites Science and Technology, 65 (2005) 281.
[14] C. Leppin, P. Wriggers, Computers & Structures, 61 (1996) 1169.
[15] J.C.J. Schellekens, R. de Borst, International Journal for Numerical Methods in Engineering, 36 (1993) 43.
[16] H.D. Espinosa, P.D. Zavattieri, Mechanics of Materials, 35 (2003) 365.
[17] O.C. Zienkiewicz, R.L. Taylor, The Finite Element Method, 5th ed., Butterworth-Heinemann, Oxford and Boston, (2000).
[18] E.O. Hall, Proceedings of the Physical Society of London B, 64 (1951) 747.
[19] N.J. Petch, Journal of the Iron Steel Institute of London, 173 (1953) 25.
[20] C.B. Hirschberger, S. Ricker, P. Steinmann, N. Sukumar, Engineering Fracture Mechanics, 76 (2009) 793.

[21] K. Matous, M.G. Kulkarni, P.H. Geubelle, Journal of the Mechanics and Physics of Solids, 56 (2008) 1511.
[22] M.G. Kulkarni, K. Matous, P.H. Geubelle, International Journal for Numerical Methods in Engineering, 84 (2010) 916.
[23] Y. Zhou, U. Erb, K.T. Aust, G. Palumbo, Scripta Materialia, 48 (2003) 825.